Materials Letters 163 (2016) 205–208

Contents lists available at ScienceDirect

Materials Letters

journal homepage: www.elsevier.com/locate/matlet

Field-directed chaining of nanowires: towards transparent electrodes

Mahshid Sam, Nima Moghimian, Rustom B. Bhiladvala *

Department of Mechanical Engineering, IESVic and CAMTEC, University of Victoria, Victoria, BC, Canada

ARTICLE INFO

Article history:
Received 22 September 2015
Received in revised form
8 October 2015
Accepted 14 October 2015
Available online 23 October 2015

Keywords:
Nanowire chain
Dielectrophoresis
Flexible substrate
Transparent electrode

ABSTRACT

Nanowire networks on rigid or flexible substrates can be used as low-cost transparent electrodes for displays, photovoltaics and as sensors. Generating an ordered configuration of connected nanowires from disordered suspension requires external forces. We demonstrate chaining of nanowires, using an AC electric field to generate dielectrophoretic force on nanowires adjacent to the electrodes and dipole–dipole interaction between nanowires far from the electrodes. Classifying and controlling forces and parameters that disrupt chaining, we provide guidelines to enable large-area coverage with multiple nanowire chains. Compared with other low-cost techniques such as spray or spin coating, AC electric field-directed assembly provides control over density and connectivity of nanowire chains with potential for fabricating low-cost, high-performance devices.

1. Introduction

Covering large surface area with connected nanowires (NWs) is of interest for fabricating devices such as light-emitting diodes (LEDs), liquid crystal displays and solar cells [1,2]. Several assembly process such as drop casting [3,4] spray [5], electrospinning [6] and nanoimprinting [7] have been used for NW network fabrication but not all assembly processes offer the combination of speed, simplicity and low cost required for technologically feasible applications. Due to the low fabrication cost of drop casting [3,4] and NW spray [5], these methods have received the most attention. However, it is difficult to achieve high coating reproducibility using these methods, since there is no director force for connecting NWs. Furthermore, in solution-processing techniques, annealing is required to remove the additives used for preventing agglomeration. This is not required in field-directed chaining.

Dielectrophoresis [8] (DEP), a force exerted on a polarizable particle in a non-uniform electric field, has been introduced as a cost-effective technique that can direct single NWs [9,10] to predetermined locations on a substrate. Moreover, it also enables NW and nanoparticle (NP) chaining between electrodes [11–15]. Simplicity, ability to direct nanostructures to desired places and a high level of end-to-end registry of nanostructures facilitate fabrication of portable and accurate devices such as gas [16] and biomolecule [17] sensors by using DEP.

However, covering a large surface area with DEP-assisted multiple NW chains is challenging. Capillary force at the drying front of the suspension [11] or electrical short circuit after connection of the first chain with assembly electrodes can disrupt chain formation. In this letter, we demonstrate how to overcome disruptive effects to create a network of NWs over a large surface area. Parameter values that enable growth of multiple long chains with reproducible configuration are specified following a discussion of the differences between field-directed assembly of single and chained NWs.

2. Materials and methods

In this work, rhodium (Rh) NWs were chained between interdigitated assembly-electrodes (see Figure S1) with different gap sizes of 180 and 240 μm. The electrodes were fabricated using 10 nm Cr/100 nm Au metal lift-off on a silicon substrate. Rh NWs were electrodeposited in porous aluminum oxide templates of 200 nm nominal pore size and 60 μm thickness (Whatman), at −400 mV with respect to a Ag/AgCl reference electrode, from an aqueous rhodium sulfate solution (RH221D from Technic) with 60 mM concentration of elemental rhodium. To extract the NWs, sections of the template were placed within a test tube containing 3 M NaOH. After 15 min of sonication, the aluminum oxide membrane was dissolved. Following this, the suspension was centrifuged and supernatant NaOH solution discarded. NWs were then rinsed with DI water and ethanol and finally suspended in ethanol [18].

NW suspension with concentration of 3.3×10^8 NW/mL was introduced over the substrate while an AC electric potential of 5 V (*rms*) and 10 kHz was applied. To create multiple NW chains bridging the electrodes, we increased the alcohol evaporation time

* Corresponding author. Fax: +1(250)721 6051.
E-mail address: rustomb@uvic.ca (R.B. Bhiladvala).

http://dx.doi.org/10.1016/j.matlet.2015.10.059
0167-577X/

by using a dam. Several parallel wells were machined within a 2-mm thick polycarbonate sheet to serve as the dam (pictured in Figure S2). Adding NW suspension (100 and 120 μL respectively, over substrates with 180 and 240 μm electrode gap sizes) we observed NW chains covering the entire substrate.

Resistance of the NWs was measured using a DC voltage applied across the NW chaining electrodes and an external resistance in series. The voltage drop across the external resistance was first used to determine the current in the circuit. The voltage drop across the electrodes with chained NWs was then measured using a probe station, and used to calculate the NW chains' resistance, without the effect of leads resistance. These data were used to construct an I–V (current versus voltage) curve.

3. Results and discussion

In single NW positioning [9], assembly-electrode gap size (L_{gap}) is comparable with NW length (L_{NW}) (Fig. 1(a)), the gradient of electric field is high within the gap and DEP is the dominant force anywhere inside the gap. However, in NW chaining [13–15], when L_{gap} is much larger than L_{NW} (20–25 times in our work), we may anticipate two different regions as shown in Fig. 1(b). (1) A region of high DEP force, adjacent to assembly electrodes, where DEP force directs NWs towards the edge of the electrodes. These edge-NWs become new electrodes with high electric field gradient at their end. (2) A region of low DEP force, in the inter-electrode space, in which polarized NWs may chain together via dipole-dipole interaction. We observed that these small chains move towards the electrodes, where they link to the edge-NWs and create a longer chain.

Based on observed phenomena, we classify chaining into three stages. (1) *Initiation*: NWs are propelled towards electrode edges, and simultaneously, small chains are generated parallel to the field between the electrodes. (2) *Growth*: when the linear density of edge-NWs has stabilized, these NWs serve as new initiators, and growth of NW chains is observed. (3) Bridging: elongated chains growing from counter electrodes meet and connect.

From initiation to bridging, several factors and forces are involved that can disrupt formation of long chains. The disruptors and guidelines to control them, are discussed below.

3.1. Effect of disruptors on chain formation

Disruptive effect of capillary force at the drying front can destroy NW chains when the generated electric field is small. At V_{rms} = 5 V, some of the chains for L_{gap}=240 μm were destroyed by capillary force at the drying front of NW suspension but no chain destruction was observed for L_{gap}=180 μm (Fig. 2(a) and (b)). One approach to overcome the capillary disruptor is to increase the voltage, thus increasing the electric field. For NWs, $F_{DEP} \propto \varepsilon_m \mathrm{Re}[F_{CM}] \nabla(E^2)$ where F_{DEP} is the DEP force and E is the electric field. Re[F_{CM}], the real part of Clausius–Mossotti factor, is equal to $(\varepsilon_m^* - \varepsilon_p^*)/\varepsilon_m^*$ where $\varepsilon^* = \varepsilon - j(\sigma/\omega)$. Subscripts m and p refer to medium and particle. ε and σ are the permittivity and conductivity, respectively, and $\omega = 2\pi f$ is the frequency of applied voltage [8]. Although increasing voltage can increase the electric field, which results in stronger field-generated forces for NW chaining, high voltage can become a disruptor unless a sufficiently high number of NWs is provided, as explained below.

When the voltage is applied, edge-NWs, positioned along the assembly electrodes, screen the electric field in their immediate neighborhood, reducing the field strength, which determines the lateral spacing between positioned NWs [19]. Higher applied voltage reduces the NW spacing, with more NWs used up in the initiation step. This results in fewer NWs being available for the growth and bridging steps, as seen in Fig. 3(a) and (b). Increasing the volume of NW suspension over the substrate prevents this disruption, creating more NW chains bridging the electrodes.

In addition to the magnitude of the applied voltage, its frequency also affects NW chaining. Two disruptors could result from inappropriate choice of applied frequency, electroosmotic force and electrode polarization [20,21]. These effects result from the presence of an electrical double layer on the surface of assembly electrodes, at frequencies lower than the relaxation frequency of the ions and the polar molecules in suspension. Frequencies higher than relaxation frequency are required to prevent double layer formation and halt the disruptive effect of electroosmosis and electrode polarization. For the assembly-electrode gap sizes and the NW medium used in this work, the ratio between the effective voltage available in the bulk of the medium and applied voltage (V_{eff}/V_{rms}) approaches unity at frequencies higher than 10 kHz. This suggests a negligible thickness of the double layer at these frequencies. Increasing the frequency above 10 kHz is not favorable for NW chaining since F_{DEP} decreases.

Chain growth and bridging can be arrested by another disruptor, a short circuit, which occurs when the first chain ends make contact with both assembly electrodes. A thin layer of dielectric deposited over the electrodes would prevent short circuits, but also isolate NW chains from the electrodes, which is undesirable. Another approach would be to coat NWs with a thin layer of dielectric material [22]. However, this would lead to an undesirable and large increase in the NW–NW contact resistance and hence chain resistance. How can we assemble NW chains and bridge assembly electrodes without an electrical short circuit?

In the suspension, a cloud of counter ions adjacent to the substrate and around each pole of the NWs, creates a repulsive electrostatic force, which repels NWs away from the electrodes. A balance between electrostatic repulsion force and DEP attraction force would make NW chains hover above electrodes [19] (gauged by the absence of short circuit). With the large gap sizes chosen to make long chains, we observed that NW chains hovered over electrodes even at 7 V rms, the maximum voltage available to us. Using a dam, NW suspension was replenished in the wells before alcohol dried out completely. Fig. 3(c) shows that although some

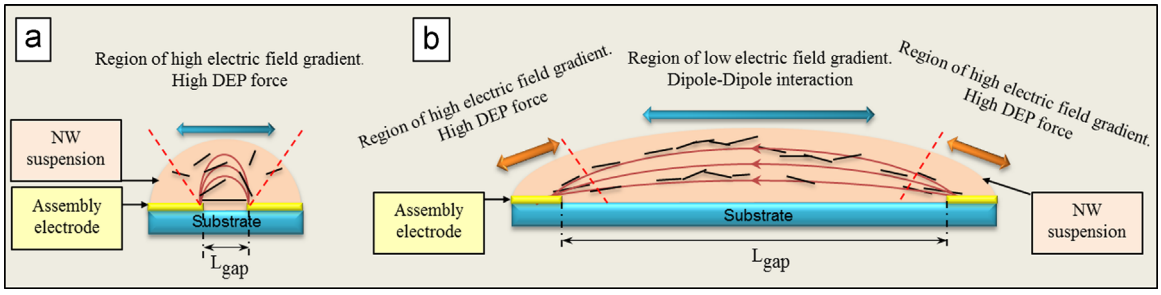

Fig. 1. Sketch of (a) single NW positioning ($L_{gap}/L_{NW} < 2$) and (b) NW chaining ($L_{gap}/L_{NW} \geq 20$).

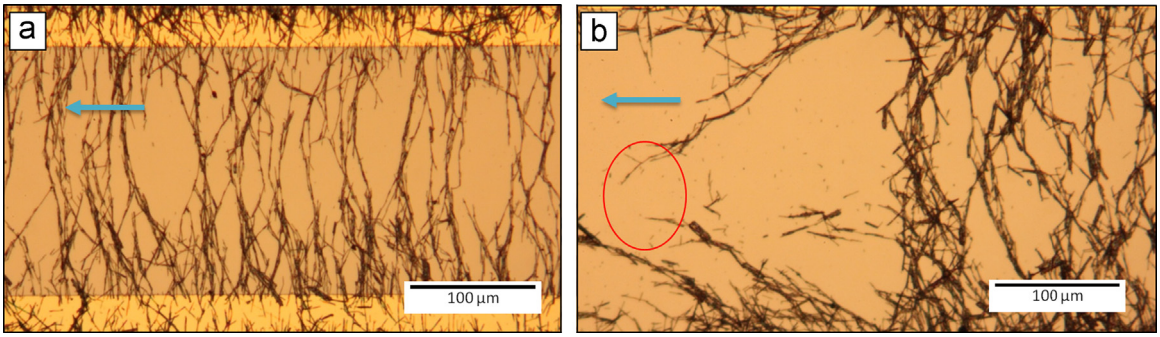

Fig. 2. (a) L_{gap} = 180 µm (b) L_{gap} = 240 µm. In (b), capillary force ruptures the bridged chains (marked with circle). The direction of motion for the drying front of the medium is indicated by the arrow.

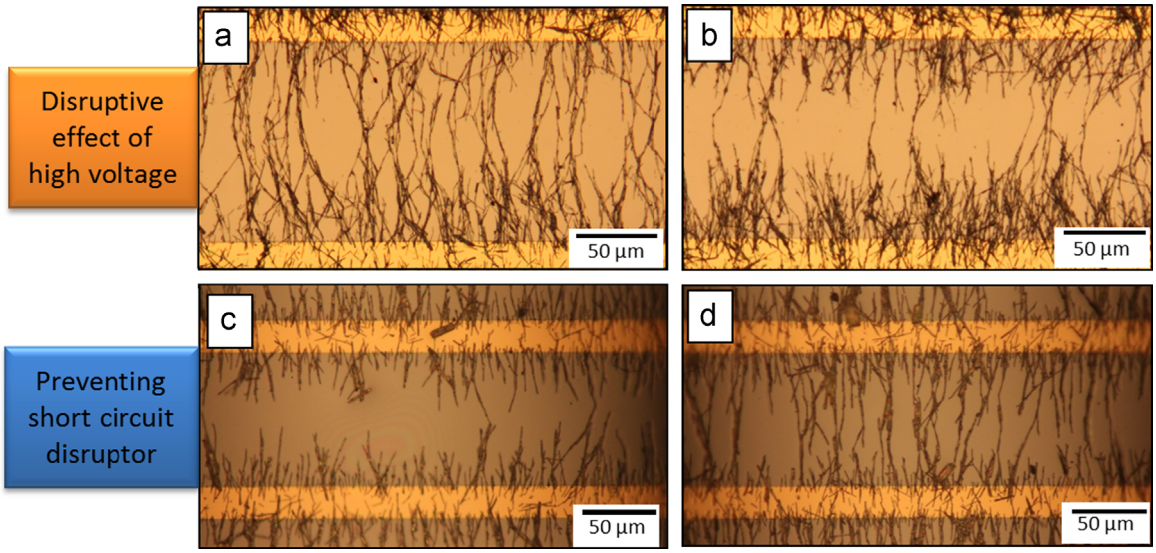

Fig. 3. Disruptor results: effect of increasing voltage from (a) V_{rms} = 5 V to (b) 7 V. (c) and (d) hovering NWs prevent a short circuit.

chains bridged the electrodes, more bridging occurred by adding NW suspension before alcohol dried out (Fig. 3(d)). Upon drying, DEP and van der Waals forces pin the NWs to the substrate.

After assembly, we examined electrical characteristics of NW chains generated for gap sizes between L_{gap} = 180 and 240 µm at 5 V (rms) and 10 kHz. The resistance measured from current-voltage (I–V) characteristics (Fig. 4) was 16 and 42 Ω for chains with gap lengths L_{gap} = 180 and 240 µm respectively. Further investigation can be undertaken to improve the electrical conductance by sintering the NWs [23,24].

The aim of this study is to generate multiple chains of NWs covering large surface area. Longer chains or large values of L_{gap} are desirable as they reduce the fraction of area covered by assembly electrodes. This can help increase the transparency of the substrate, as needed for electrode applications. To the best of our knowledge, the longest field-assisted chain was a 3 mm *single* chain of gold NPs [25]. The method demonstrated here enables coverage of large surface area with *multiple* long chains, without the disruptive effect of a short circuit. By choosing parameter values that provide a large enough director force and prevent disruptors, field-directed chaining of NWs provides a path to create reproducible properties (such as electrical conductivity and light transmissivity) over large surface area and with low fabrication cost.

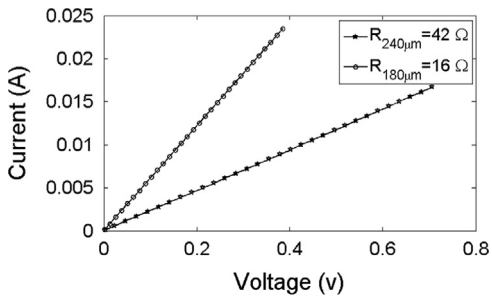

Fig. 4. Resistance measurement for chains of L_{gap} = 180 and 240 µm.

4. Conclusions

We showed that field directed NW chaining between gaps much larger than NW-length, differs from that for single NW assembly between gaps comparable to nanowire length. While dielectrophoresis is the predominant force for single NW positioning, for nanowire chaining its influence dominates for only a small fraction of the gap region, close to the electrodes. In the region far from the electrodes, dipole-dipole interaction is dominant. Lower electric-field strength in nanowire chaining can make nanowire chains hover above assembly electrodes and prevent electrical short circuits, which enables the covering of large surface area with multiple chains. Forces and parameters that can disrupt NW chaining were noted as capillary force, high voltage with an insufficient number of nanowires, electro-osmotic velocity, electrode polarization and a short circuit. Guidelines to control them were presented.

This method is not limited by the dimension of the substrate or size and type of polarizable NWs and should help in the development of scalable and cost effective techniques for making sensors and optoelectronic devices.

Acknowledgments

This work was supported by Canadian agencies NSERC, CFI and BCKDF and made use of the 4D LABS facilities at Simon Fraser University.

Appendix A. Supplementary data

Supplementary data associated with this paper can be found in the online version at http://dx.doi.org/10.1016/j.matlet.2015.10.059.

References

[1] D.H. Kim, N. Lu, R. Ghaffari, J.A. Rogers, Inorganic semiconductor nanomaterials for flexible and stretchable bio-integrated electronics, NPG Asia Mater. 4 (4) (2012) e15.
[2] K. Ellmer, Past achievements and future challenges in the development of optically transparent electrodes, Nat. Photon. 6 (12) (2012) 809–817.
[3] J.Y. Lee, S.T. Connor, Y. Cui, P. Peumans, Solution-processed metal nanowire mesh transparent electrodes, Nano Lett. 8 (2) (2008) 689–692.
[4] L. Hu, H.S. Kim, J.Y. Lee, P. Peumans, Y. Cui, Scalable coating and properties of transparent, flexible, silver nanowire electrodes, ACS Nano 4 (5) (2010) 2955–2963.
[5] P.N. Nirmalraj, A.T. Bellew, A.P. Bell, J.A. Fairfield, E.K. McCarthy, C. OKelly, L. F. Pereira, S. Sorel, D. Morosan, J.N. Coleman, Manipulating connectivity and electrical conductivity in metallic nanowire networks, Nano Lett. 12 (11) (2012) 5966–5971.
[6] H. Wu, D. Kong, Z. Ruan, P.C. Hsu, S. Wang, Z. Yu, T.J. Carney, L. Hu, S. Fan, Y. Cui, A transparent electrode based on a metal nanotrough network, Nat. Nanotechnol. 8 (6) (2013) 421–425.
[7] M.G. Kang, M.S. Kim, J. Kim, L.J. Guo, Organic solar cells using nanoimprinted transparent metal electrodes, Adv. Mater. 20 (23) (2008) 4408–4413.
[8] T.B. Jones, Electromechanics of Particles, Cambridge University Press, New York, 1995.
[9] M. Li, R.B. Bhiladvala, T.J. Morrow, J.A. Sioss, K.K. Lew, J.M. Redwing, C. D. Keating, T.S. Mayer, Bottom-up assembly of large-area nanowire resonator arrays, Nat. Nanotechnol. 3 (2) (2008) 88–92.
[10] J.A. Sioss, R.B. Bhiladvala, W. Pan, M. Li, S. Patrick, P. Xin, S.L. Dean, C.D. Keating, T.S. Mayer, G.A. Clawson, Nanoresonator chip-based RNA sensor strategy for detection of circulating tumor cells: response using PCA3 as a prostate cancer marker, Nanomed.: Nanotechnol. Biol. Med. 8 (6) (2012) 1017–1025.
[11] K.H. Bhatt, O.D. Velev, Control and modeling of the dielectrophoretic assembly of on-chip nanoparticle wires, Langmuir 20 (2) (2004) 467–476.
[12] R. Kretschmer, W. Fritzsche, Pearl chain formation of nanoparticles in microelectrode gaps by dielectrophoresis, Langmuir 20 (26) (2004) 11797–11801.
[13] D.L. House, H. Luo, S. Chang, Numerical study on dielectrophoretic chaining of two ellipsoidal particles, J. Colloid Interface Sci. 374 (1) (2012) 141–149.
[14] A. Oliva-Avilés, F. Avilés, V. Sosa, G. Seidel, Dielectrophoretic modeling of the dynamic carbon nanotube network formation in viscous media under alternating current electric fields, Carbon 69 (2014) 342–354.
[15] W. Ahmed, E.S. Kooij, A. Van Silfhout, B. Poelsema, Quantitative analysis of gold nanorod alignment after electric field-assisted deposition, Nano Lett. 9 (11) (2009) 3786–3794.
[16] S. Ghashghaie, E. Marzbanrad, B. Raissi, C. Zamani, R. Riahifar, Effect of low frequency electric field parameters on chain formation of ZnO nanoparticles for gas sensing applications, J. Am. Ceram. Soc. 95 (6) (2012) 1843–1850.
[17] S. Cherukulappurath, S.H. Lee, A. Campos, C.L. Haynes, S.H. Oh, Rapid and sensitive in situ SERS detection using dielectrophoresis, Chem. Mater. 26 (7) (2014) 2445–2452.
[18] N. Moghimian, M. Sam, R.B. Bhiladvala, Rhodium nanowires: synthesis and nanostructure tailoring by controlling hydrogen evolution, Mater. Lett. 113 (2013) 152–155.
[19] S.J. Papadakis, J.A. Hoffmann, D. Deglau, A. Chen, P. Tyagi, D.H. Gracias, Quantitative analysis of parallel nanowire array assembly by dielectrophoresis, Nanoscale 3 (3) (2011) 1059–1065.
[20] N.G. Green, A. Ramos, A. Gonzalez, H. Morgan, A. Castellanos, Fluid flow induced by nonuniform ac electric fields in electrolytes on microelectrodes. I. Experimental measurements, Phys. Rev. E 61 (4) (2000) 4011–4018.
[21] B.C. Gierhart, D.G. Howitt, S.J. Chen, R.L. Smith, S.D. Collins, Frequency dependence of gold nanoparticle superassembly by dielectrophoresis, Langmuir 23 (24) (2007) 12450–12456.
[22] S. Boehm, L. Lin, K. Guzman Betancourt, R. Emery, J. Mayer, T. Mayer, C. D. Keating, Formation and frequency response of two-dimensional nanowire lattices in an applied electric field, Langmuir 31 (2015) 5779–5786.
[23] E.C. Garnett, W. Cai, J.J. Cha, F. Mahmood, S.T. Connor, M.G. Christoforo, Y. Cui, M.D. McGehee, M.L. Brongersma, Self-limited plasmonic welding of silver nanowire junctions, Nat. Mater. 11 (3) (2012) 241–249.
[24] J.A. Spechler, K.A. Nagamatsu, J.C. Sturm, C.B. Arnold, Improved efficiency of hybrid organic photovoltaics by pulsed laser sintering of silver nanowire network transparent electrode, ACS Appl. Mater. Interfaces 7 (2015) 10556–10562.
[25] S.O. Lumsdon, D.M. Scott, Assembly of colloidal particles into microwires using an alternating electric field, Langmuir 21 (11) (2005) 4874–4880.